

1 **A vertical transport window of water vapor in the troposphere**
2 **over the Tibetan Plateau with implication for global climate**
3 **change**

4
5 **Xiangde Xu^{1,2}, Chan Sun^{1,2}, Deliang Chen³, Tianliang Zhao^{1*}, Jianjun Xu⁴,**
6 **Shengjun Zhang², Juan Li¹, Bin Chen², Yang Zhao², Hongxiong Xu², Lili Dong²,**
7 **Xiaoyun Sun¹, Yan Zhu¹**

8
9 ¹ Nanjing University of Information Science and Technology, Nanjing 210044, China;

10 ² State Key Laboratory of Severe Weather, Chinese Academy of Meteorological Sciences,
11 Beijing, 100081, China;

12 ³ Regional Climate Group, Department of Earth Sciences, University of Gothenburg,
13 Sweden;

14 ⁴ South China Sea Institute of Marine Meteorology, Guangdong Ocean University,
15 Zhanjiang 524088, China

16 * Corresponding author. **Email:** tlzhao@nuist.edu.cn

17

18

19

20

21 **Abstract**

22 By using the multi-source data of meteorology over recent decades, this study
23 discovered a summertime “hollow wet pool” in the troposphere with a center of high
24 water vapor over Asian water tower (AWT) on the Tibetan Plateau (TP), which is
25 featured by a vertical transport “window” in the troposphere. The water vapor transport in
26 the upper troposphere extends from the vertical transport window over the TP with the
27 significant connections among the Arctic, Antarctic and TP regions, highlighting the
28 effect of TP’s vertical transport window of water vapor in the troposphere on global
29 change of water vapor. The vertical transport window is built by the AWT’s thermal
30 forcing in association with the dynamic effect of the TP’s “hollow heat island”. Our
31 study improves the understanding on the vapor transport over the TP with an important
32 implication to global climate change.

33

34

35 **1. Introduction**

36 The Tibetan Plateau (TP) is the largest high terrain in the world, known as "the roof
37 of the world" with an averaged altitude over 4,000 meters. The rivers, such as the
38 Yangtze River, Yellow River, Lancang River and Ganges River, are all originated from
39 the TP, which is regarded as the "Asian Water Tower" (AWT) (Xu et al., 2008). The
40 three-river-source (Yangtze, Yellow, and Lancang Rivers) region (TRSR) in the eastern
41 TP is the core area of the AWT over the plateau (Xu et al., 2014). The observed "CISK-
42 like mechanism" is an important mechanism sustaining the atmospheric "water tower"
43 over the AWT (Xu et al., 2014). Connecting with the cloud and precipitation in the AWT,
44 the plausible hydrological cycles could be realized with the transport of water vapor from
45 tropical oceans up to the TP (Xu et al., 2014).

46

47 Water vapor plays an important role in global environment and climate changes
48 (Tian et al.,2009; Solomon et al.,2010). The ratio of strong convective clouds to total
49 clouds over the Tibetan Plateau (TP) is about 5 times to the global ratio, and the frequent
50 occurrences of strong convective clouds could be largely attributed to the TP's large
51 topography (Luo et al.,2011; Su et al.,2006). The water vapor in the upper troposphere is
52 mainly originated from the tropical lower troposphere through vertical transport and
53 evaporation of convectively transported or in situ produced cloud ices (Tian et al.,2004;
54 James, et al.,2008). Water vapor was first lifted by convection over the Bay of Bengal
55 and the South China Sea and then transported upwards the tropical tropopause layer via
56 the monsoon anticyclonic circulations towards Northwest India (Yanai, et al., 1973; Chen,

57 et al., 2012). TP is a moisture sink in summer, having a net moisture convergence of 4
58 mm each day, where the convergences were enhanced from 1979 to 2018 (Feng and
59 Zhou, 2012; Xu, et al., 2020). In general, Asian monsoon circulation provides an
60 effective pathway for regional water vapor transport to the TP (Wang, et al.,2017). An
61 important role of the anticyclone over the TP is verified in the exchange of water vapor
62 between the troposphere and stratosphere (Garny, et al., 2016; Fu, et al., 2006) . Many
63 studies have been focused on the transport of water vapor into upper troposphere and
64 lower stratosphere from the tropical oceans to the high-altitude TP (Chen, et al., 2012;
65 Wang, et al.,2017; Xie, et al.,2018; Randel, et al.,2013). However, inadequate attention
66 has been paid to the vertical transport of water vapor in the troposphere over the TP,
67 especially in respect of the underlying mechanism and the consequences on global
68 climate.

69

70 The following questions are of great concern in the TP' vertical transport of water
71 vapor study with the implication for global change, for example, what is the formation
72 mechanism on the vertical transport window of water vapor in the troposphere on the TP?
73 How is the vertical transport of water vapor in the troposphere constructed with the
74 special column of apparent heat source in the AWT over the TP ? How is the global
75 effect of the vertical transport window of water vapor in the troposphere on the TP?
76 From the perspective of global atmospheric energy and water vapor exchanges, this study
77 characterizes a window of water vapor vertical transport within the troposphere over the
78 TP and the implication for global change.

79

80 **2. Data and Methods**

81 The daily meteorological data of cloud amount are provided by the meteorological
82 observatories in the TP in the period of 1979 to 2018. The AIRS remote sensing products
83 of water vapor from 2003 to 2018 and the ECMWF-interim data of meteorology from
84 1979 to 2018 are used in this study.

85

86 In this study, the inverse algorithm is used to calculate the apparent heat source Q_1 ,
87 and the formula is as follows (Su et al.,2006) :

88
$$Q_1 = C_p \left[\frac{\partial T}{\partial t} + \vec{V} \cdot \nabla T + \left(\frac{p}{p_0} \right)^k \bar{\omega} \frac{\partial \theta}{\partial p} \right] \quad (1)$$

89 where T is the air temperature; ω is the vertical velocity at the p coordinate,
90 $P_0 = 1000$ hPa; $k = R/C_p$; V is the horizontal wind vector; θ is the potential temperature.

91 Vertical integration of Q_1 is expressed as:

92
$$\langle Q_1 \rangle = \frac{1}{g} \int_{p_t}^{p_s} Q_1 dp \quad (2)$$

93 where p_s is the surface air pressure, and p_t is the top air pressure, here taken as 300hPa.

94

95 In order to analyze the relationship between water vapor sources and vapor
96 transport channels in the atmospheric water cycle, the correlation vector calculation was
97 used to calculate the temporal and spatial variations of the water vapor transport channels.

98 The expression is:

99
$$\vec{R}(x, y) = R_u(x, y)i + R_v(x, y)j \quad (3)$$

100 where $\vec{R}(x,y)$ represents the correlation vector in which $R_u(x, y)$ represents the
101 correlation coefficients between water vapor and the component of latitudinal water
102 vapor flux qu , and $R_v(x, y)$ represents correlation coefficients between water vapor and
103 longitudinal water vapor flux components qv .

104

105 **3. Results and discussion**

106 **3.1 The structures of vertical transport window of water vapor over the TP**

107 With the use of satellite remote sensing products from 2003 to 2016, the global
108 distribution of the total water vapor from 500hPa to 300hPa in the troposphere was
109 shown in Figure 1a . The results indicate that there is a high value center of water vapor
110 in the mid- and upper troposphere over the TP, extending southwards to the Bay of
111 Bengal, India and Northern Southeast Asia. It is worth noting that the fraction of strong
112 convective clouds to the total cloud ranges from 4.0 % to 21.0 % in the TP, and during
113 the summer season the thermal forcing of TP is dominated by the latent heat released by
114 cloud and precipitation (Fu et al.,2006; Dessler et al.,2006; Gao et al.,2014). The intense
115 mesoscale convective activity, which is represented with the low cloud fraction based on
116 the cloud characteristics observed in the TP, and the "massive chimney effect" of huge
117 cumulonimbus cloud drive the transport of atmospheric heat and water vapor to the upper
118 troposphere (Fu et al.,2006; Xie et al.,2018). Based on Chinese Third Tibetan Plateau
119 Experiment-Observation of Boundary Layer and Troposphere (2014–2017), it is observed
120 in the TP that the cloud-top height was averaged around 11.5 km (a.s.l.) with its

121 maximum value exceeding 19 km (a.s.l.) , and the mean cloud-base height at 6.88 km
122 (a.s.l.) during the observation period, reflecting the TP's deep convection in the
123 troposphere and its impact on the upper troposphere.

124

125 **3.2 Global effect of the vertical transport window over the TP**

126 The vertical section of the correlation coefficients along the south-north direction
127 between the low cloud cover on the TP and the global water vapor are presented in
128 Figure 1b. The obviously upward movement of water vapor over the TP can be seen in
129 Figures 2a. It could be noticed that there exist the structures similar with the massive
130 chimney between the convective cloud and the water vapor on the TP (Figures 1b and
131 2a). Figures 2b and 2c show significant correlation between convective clouds over the
132 AWT and the changes of global water vapor from 1979 to 2018. Significant correlations
133 extend from the TP southward and northward in the upper troposphere. It is remarkable
134 that the high correlation areas passing the 90% confidence level expand towards the polar
135 regions of both the southern and the northern hemispheres (Figures 1b, 2b and 2c),
136 depicting the relation between the convective clouds and the global water vapor in the
137 upper troposphere across the northern and southern hemispheres for an implication of the
138 TP to global climate change.

139 The distributions of high positive correlation coefficients between low cloud
140 cover over the TP and the global water vapor in the upper troposphere are calculated by
141 ECMWF-interim reanalysis data (Figure 3a). It can be found that there is a region with
142 highest values of correlation coefficients in the upper troposphere (500hPa-300hPa),
143 covering a banded large area from the plateau across the lower latitude tropical zone to

144 the polar regions, indicating the significant correlations between convective cloud
145 activities on the TP and the global water vapor in the upper troposphere, especially in the
146 polar region of the southern hemisphere area (Figure 3a), which could be reflected an
147 importance of the thermal forcing of TP in global changes of water vapor.

148 The strong anticyclone in the upper troposphere over the southeastern TP takes a
149 significant part in the upward transport of water vapor in the troposphere and stratosphere
150 (Garny, et al., 2016; Fu, et al., 2006). In order to understand the effect of the vertical
151 transport window of troposphere over the TP on the global water vapor distribution from
152 the perspective of the dynamic effect of anticyclone over the plateau driven by the heat
153 sources, we presented the distributions of correlation coefficients between daily mean Q_1
154 in the TP and global water vapor flux in July from 2014 to 2016 at 300hPa (fig. 3b.)
155 Driven by the heat source of the TP, the anticyclone is formed in the upper troposphere
156 over the TP and surrounding regions, which governed the water vapor transport from the
157 TP not only to the surrounding area, but also extending to the north and south poles along
158 the long-range transport channels (Fig. 3b), which indicates the vertical transport window
159 effect of the TP on global water vapor transport, especially over high-latitude regions
160 such as the Arctic and Antarctic. To further verify the global transport pathways of water
161 vapor from the TP, we used the methods of composite analysis to characterize global
162 distribution of water vapor transport fluxes at the 300hpa in the years to anomalously
163 high and low Q_1 over the TP. The TP's anticyclone in the upper troposphere is often
164 associated with deep convection in the troposphere (Garny, et al., 2016). Fig. 3c
165 shows that in years with higher Q_1 , stronger anticyclone formed at the upper troposphere
166 (Fig. 3b), which maintains the upward transport of water vapor to the upper troposphere,

167 with strong transport of water vapor transport the arctic and antarctic (Fig. 3c),
168 confirming the impact of the vertical transport in the troposphere driven by heat released
169 within AWT in the TP on global water vapor transport especially to the polar regions.

170 The Indian continent heats up from spring to summer, hence the convection draws
171 moisture northwards from the Bay of Bengal, Arabian Sea and Indian Ocean, leading to
172 precipitation in the Himalayas and beyond (Yanai et al., 1973). In Figure 3d, it could be
173 found that, driven by the strong apparent heat source, the water vapor flows from the low
174 latitude ocean could build a remarkable channel to the TP. The key entrance to the water
175 vapor passage is just the intersection of the Himalayas on the southern slope of the TP.
176 This region constitutes a special canyon pass in the plateau with deep valleys, making a
177 perfect entrance zone for the oceanic warm-wet water flows (see the terrain distribution
178 inserted in the lower right corner of Figure 3d).

179 FLEXPART trajectory model (Stohl, et al., 2005; Reale, et al 2001; James, et al, 2004)
180 was used to simulate the spatial and temporal changes of water vapor transport to the
181 TRSR over the TP, driven with the ERA-Interim reanalysis data of meteorology with
182 horizontal resolution of $0.75^{\circ} \times 0.75^{\circ}$ in July 2009. In the FLEXPART particle diffusion
183 model, the 80000 particles was released at the TRSR (90° - 102° E and 30° - 35° N). In
184 Figure 3f, it can be found that the water vapor in the TRSR was traced to water vapor
185 source on the tropical Indian Ocean. The water vapor from the central Indian Ocean in
186 the southern hemisphere can be transported along the Somali jet flow through the
187 Arabian Sea to the TP. The water vapor from the South China Sea and the Bay of Bengal
188 was transported to the TP converging over the TRSR (Figure 3f), characterizing the water
189 vapor transport channel from the southern hemispheric and low latitude oceans to the TP. |

190 According to the correlation analysis of water vapor transport, the water vapor
191 source of the AWT can also be traced back to the ocean surface water vapor source
192 region with water vapor positive correlation extreme value region in the Chagos
193 Archipelago of the Central Indian Ocean near 10°S south of the equator (Figure 3e),
194 revealing that the TP is the confluence area of the hemispherical water vapor from the
195 southern Indian Ocean.

196

197 **3.3 The transport window of water vapor driven by the AWT**

198 Through the correlation analysis of the column apparent heat Q_1 over the TP as
199 well as the three-dimensional structure of vorticity and divergence, it can be found that
200 the apparent heat source Q_1 in the TP is an important forcing factor (Figure 4). The
201 results show that the air heat island in the AWT is located at 300-500 hPa in the upper
202 troposphere, which is regarded as the high apparent heat Q_1 area significantly related to
203 the convective clouds and the strong ascending movement (Figures 4a and 4d). Figures
204 4b,4c, 4e and 4f present the correlations of the column apparent heat Q_1 in AWT with the
205 divergence and vorticity fields over the TP, which can describe the effective "suction
206 effect" with divergence (negative vorticity) at upper levels and convergence (positive
207 vorticity) at lower levels in the troposphere. The Q_1 is significantly released in the
208 convective clouds and the strong ascending movement, and there exists a strong
209 anticyclonic circulation in the upper troposphere over the region of the AWT in the
210 southeast of the plateau (Figure 3b). In addition, the lower troposphere is the center of
211 strong convergence and strong vorticity. Figure 3g shows the difference of vapor
212 transport flux and specific humidity at 500hPa in summer between anomalously high and

213 low Q_1 . When the Q_1 in TRSR is anomalously high, large water vapor from the tropical
214 oceans is transported across the Bay of Bengal and the Indian peninsula, and entered the
215 TP from the southern edge, revealing the TP's thermal effect could make a strong vapor
216 transport channel connecting the water vapor source in the low latitude tropical oceans.

217

218 All these results reveal the effective "pumping effect" of the vertical configuration
219 with low-level cyclonic circulation and high-level divergence with anticyclone
220 circulation over the TP. The strong confluence effect building the vertical transport
221 window of water vapor could be driven by the elevated heating on the TP in the
222 troposphere with the water vapor flow, making a strong vapor transport connecting the
223 water vapor source in the low latitude oceans with the high water vapor center over the
224 core area of AWT over the TP. The water vapor transport connect from the vertical
225 transport window over the TP and the Arctic, Antarctic regions in the upper troposphere,
226 highlighting the effect of TP "hollow wet pool" on global climate change.

227 **4. Conclusion**

228 By using the multi-source data of meteorology over recent decades, this study
229 discovered a summertime "hollow wet pool" in the troposphere with a center of high
230 water vapor over AWT on the highly elevated TP, which is featured by a vertical
231 transport window with the transport flux of water vapor in the troposphere. Driven by the
232 strong TP's heat source, water vapor flows connect the AWT over the TP with the low-
233 latitude oceans. Significant correlations exist between convective activities on the TP and
234 global water vapor in the upper troposphere,. The water vapor transport from the TP's

235 vertical window in the upper troposphere extends from the TP globally towards the
236 northern and southern hemispheres with the significant connections among the three
237 poles of Arctic, Antarctic and TP regions, highlighting the effect of TP's vertical
238 transport window of water vapor on global climate change. The vertical transport window
239 is built by the AWT's thermal forcing in association with the dynamic effect of the TP's
240 "hollow heat island" as well as the effective "pumping effect" on vertical transport with
241 low-level convergences with cyclonic circulation and upper-level divergences with
242 anticyclone circulation in the troposphere over the TP.

243 Basd on this observational study, a conceptual model of the comprehensive relation
244 of the TP region with the global energy and water cycles is put forward for the vertical
245 transport window of vapor in the troposphere driven by the thermal forcing in the core
246 region of the AWT over the TP (Figure 5), where the water vapor source is traced back to
247 tropical ocnas and the Southern Hemisphere. The thermal effect of the TP could sustain
248 the vertical upward transport of the energy and water vapor. The water cycle in the AWT
249 clearly displays the linkages of the vertical transport window of water vapor in the
250 troposphere over the TP with the vapor source in the tropical oceans and the southern
251 Indian Ocean in the lower troposphere and with the Arctic and Antarctic regions in the
252 upper troposphere ((Figure 5). Our study depicts a comprehensive understanding on the
253 vertical water vapor transport in the atmosphere over the TP with an important
254 implication to global climate change.

255

256 **Data availability.** ERA-Interim of ECMWF ([https://apps.ecmwf.int/datasets/data/interim-](https://apps.ecmwf.int/datasets/data/interim-full-moda/levtype=pl/)
257 [full-moda/levtype=pl/](https://apps.ecmwf.int/datasets/data/interim-full-moda/levtype=pl/)) reanalysis daily and monthly data are part of the European Center

258 for Medium-range Weather Forecasts. AIRS Science Team/Joao Teixeira (2013),
259 AIRS/Aqua L3 Daily Standard Physical Retrieval (AIRS-only) 1 degree x 1 degree V006,
260 Greenbelt, MD, USA, Goddard Earth Sciences Data and Information Services Center
261 (GES DISC), Accessed: [Jan. 2019], 10.5067/Aqua/AIRS/DATA303. The low cloud data
262 used in this study are derived from the Data Sets of Surface Meteorological Elements in
263 China released by the National Meteorology Information Center, China Meteorological
264 Administration, which can be found at
265 <https://zenodo.org/record/5121157#.YPkRHqjitPY> (Sun, 2021).

266

267 **Author Contributions.** XDX, CS and TLZ conducted the study design. DLC, JJX and
268 SJZ analysed the observational data. JL, BC, YZ, HXX, LLD, YYS, and YZ assisted
269 with data processing. XDX, CS and TLZ wrote and revised the manuscript. XDX, CS,
270 TLZ, and JJX were involved in the scientific interpretation and discussion. All authors
271 provided commentary on the paper.

272

273 **Competing interests.** The authors declare that they have no conflict of interest.

274

275 **Acknowledgments.** The authors acknowledge the support from the The Second Tibetan
276 Plateau Scientific Expedition and Research (STEP) program and the Scientific and
277 Technological Development Funds from Chinese Academy of Meteorological Sciences.
278 We would like to thank the editor and the two anonymous reviewers, for their
279 suggestions on restructuring the initial draft.

280 **Financial support.** This study was supported by The Second Tibetan Plateau Scientific
281 Expedition and Research (STEP) program (2019QZKK0105) and the Scientific and
282 Technological Development Funds from Chinese Academy of Meteorological Sciences
283 (2021KJ022 and 2021KJ013).

284

285 **Competing interests.** The authors declare that they have no conflict of interest.

286

287 **References**

288 Chen, B., Xu, X. D., Yang, S., and Zhao, T. L.: Climatological perspectives of air transport from
289 atmospheric boundary layer to tropopause layer over Asian monsoon regions during boreal summer
290 inferred from Lagrangian approach. *Atmos. Chem. Phys.*, 12, 5827-5839. [https://doi.org/10.5194/acp-](https://doi.org/10.5194/acp-12-5827-2012)
291 [12-5827-2012](https://doi.org/10.5194/acp-12-5827-2012), 2012.

292 Dessler, A and Sherwood, S.: Effect of convection on the summertime extratropical lower stratosphere. *J.*
293 *Geophys. Res.*, 109, D23301. <https://doi.org/10.1029/2004JD005209>, 2004.

294 Feng, L., and Zhou, T.: Water vapor transport for summer precipitation over the Tibetan Plateau: Multidata
295 set analysis, *J. Geophys. Res.*, 117, D20114, doi:10.1029/2011JD017012, 2012.

296 Fu, R., Hu, Y., Wright, J., Jiang, J., H., Dickinson, R., E., Chen, M., X., Filipiak, M., Read, W., G., Waters,
297 W., W., and Wu, D., L.: Short circuit of water vapor and polluted air to the global stratosphere by
298 convective transport over the Tibetan Plateau, *Proceedings of the National Academy of Sciences of the*
299 *United States of America.*, 103, 5664-5669. <https://doi.org/10.1073/pnas.0601584103>, 2006.

300 Gao, Y, Cuo, L and Zhang, Y.: Changes in Moisture Flux over the Tibetan Plateau during 1979–2011 and
301 Possible Mechanisms. *J. Climate*, 27, 1876-1893. <https://doi.org/10.1175/JCLI-D-13-00321.1>, 2014.

302 Garny, H. and Randel, W. J.: Transport pathways from the Asian monsoon anticyclone to the stratosphere,
303 *Atmos. Chem. Phys.*, 16, 2703–2718, [https://doi.org/10.5194/acp-16-2703-](https://doi.org/10.5194/acp-16-2703-2016) 2016, 2016.

304 James, R. , Bonazzola, M. , Legras, B. , Surbled, K. , & Fueglistaler, S.: Water vapor transport and
305 dehydration above convective outflow during Asian monsoon. *Geophys. Res. Lett.*, 35, L20810.
306 <https://doi.org/10.1029/2008GL035441>, 2008.

307 James, P., Stohl, A., Spichtinger, N.: Climatological aspects of the extreme European rainfall of August
308 2002 and a trajectory method for estimating the associated evaporative source regions. *Nat Hazards*
309 *Earth Syst Sci*, 4, 733 – 746, 2004.

310

311 Luo, Y. , Zhang, R. , Qian, W. , Luo, Z. , and Hu, X.: Intercomparison of deep convection over the tibetan
312 plateau--asian monsoon region and subtropical north america in boreal summer using cloudsat/calipso
313 data. *Journal of Climate*. 24, 2164-2177, 2011.

314 Randel, W. J. & Jensen, E. J.: Physical processes in the tropical tropopause layer and their roles in a
315 changing climate. *Nat. Geosci*,6, 169. <https://doi.org/10.1038/ngeo1733>, 2013.

316 Reale, O., Feudale, L., Turato, B.: Evaporative moisture sources during a sequence of floods in the
317 Mediter-ranean region. *Geophys. Res. Lett.*, 28, 2085 – 2088, 2001.

318 Solomon, S., Rosenlof, K. H., Portmann, R. W., Daniel, J. S., Davis, S. M. , Sanford, T. J. and Plattner,
319 G. K.: Contributions of stratospheric water vapor to decadal changes in the rate of global warming.
320 *Science*, 327: 1219–1223. <https://doi.org/10.1126/science.1182488>, 2010.

321 Su, H, Read, W, Jiang, J. H. , Waters, J. W. , and Fetzer, E. J.: Enhanced positive water vapor feedback
322 associated with tropical deep convection: New evidence from Aura MLS. *Geophys. Res. Lett.*, 33.
323 <https://doi.org/10.1029/2005GL025505>, 2006.

324 Sun, C. : Low Cloud Amount, Zenodo [data set], <https://doi.org/10.5281/zenodo.5121157>, 2021

325 Stohl, A., Forster, C., Frank, A., Seibert, P. and Wotawa G.: Technical note: The Lagrangian particle
326 dispersion model FLEXPART version 6.2. *Atmos. Chem. Phys.*, 5, 2461 – 2474, DOI: 10.5194/acpd-
327 5-4739-2005, 2005.

328 Tian, B, Soden, B, Wu, X.: Diurnal cycle of convection, clouds, and water vapor in the tropical upper
329 troposphere: Satellites versus a general circulation model. *J. Geophys. Res. Atmos.*, 27, 2173-2176.
330 <https://doi.org/10.1029/2003JD004117>, 2004.

331 Tian, W. S., Chipperfield, M. and Lü, D. R.: Impact of increasing stratospheric water vapor on ozone
332 depletion and temperature change. *Adv. Atmos. Sci.* ; 26: 423–437. <https://doi.org/10.1007/s00376-009-0423-3>, 2009.

334 Wang, Y, Zhang, Y, Chiew, F., McVicar, T., R., Zhang, L., Li, H., and Qin , G.: Contrasting runoff
335 trends between dry and wet parts of eastern Tibetan Plateau, *Sci. Rep. U.K.* 7: 15458.
336 <https://doi.org/10.1038/s41598-017-15678-x>, 2017.

337 Xie, F., Zhou, X. ,Li, J. , Chen, Q. , Zhang, J. , Li, Y.,Ding, R. ,Xue, J. and Ma, X.: Effect of the Indo-
338 Pacific Warm Pool on lower stratospheric water vapor and comparison with the effect of the El Niño–
339 Southern Oscillation. *J. Clim.* 31, 929–943, <https://doi.org/10.1175/JCLI-D-17-0575.1>, 2018.

340 Xu, K., Zhong, L., Ma, Y., Zou,M., and Huang Z.: A study on the water vapor transport trend and water
341 vapor source of the Tibetan Plateau. *Theor. Appl. Climatol.*, **140**, 1031–1042,
342 <https://doi.org/10.1007/s00704-020-03142-2>, 2020.

343 Xu, X, Zhao, T, Lu C., Guo, Y., Chen, B., Liu, R., Li, Y., and Shi, X.: An important mechanism sustaining
344 the atmospheric "water tower" over the Tibetan Plateau. *Atmos. Chem. Phys.* 14, 11287-11295,
345 <https://doi.org/10.5194/acp-14-11287-2014>, 2014.

346 Xu, X., Lu, C. Shi, X. and Gao, S.: World water tower: An atmospheric perspective, *Geophys. Res. Lett.*,
347 35, L20815. <https://doi.org/10.1029/2008GL035867>, 2008.

348 Yanai, M. , Esbensen, S. , and Chu, J. H.: Determination of bulk properties of tropical cloud clusters from
349 large-scale heat and moisture budgets. *Journal of Atmospheric Sciences*, 30(4), 611-
350 627.[https://doi.org/10.1175/1520-0469\(1973\)030<0611:DOBPOT>2.0.CO;2](https://doi.org/10.1175/1520-0469(1973)030<0611:DOBPOT>2.0.CO;2), 1973.

351

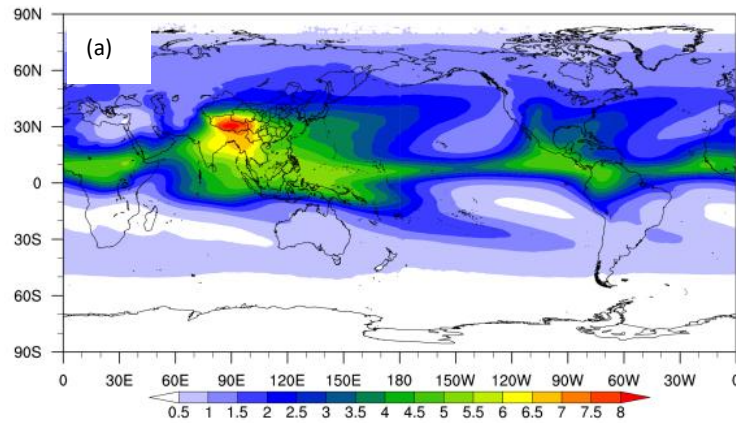
352

353

354

355

356

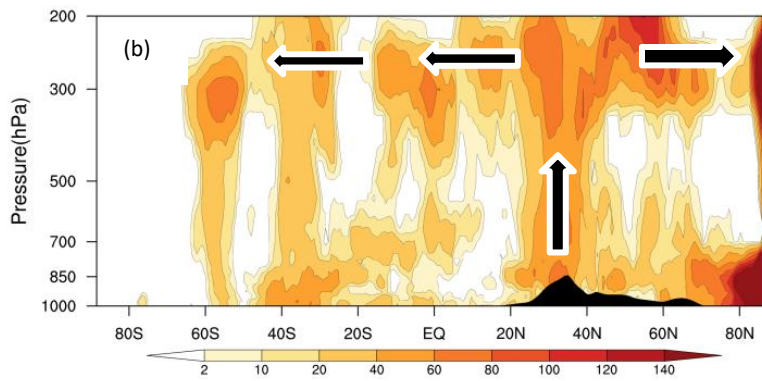


357

358

359

360



361

362 **Figure 1.** (a) The global distribution of the total water vapor from 300 hPa to 500 hPa

363 based on the summertime AIRS data from 2003 to 2018, (b) the vertical section of the

364 frequency (shaded) of the correlation coefficients passing the level of 90%

365 confidence between summertime TP's low cloud cover and the water vapor at different

366 vertical levels along the meridional direction averaged over 60°E - 180°E for 1979-

367 2016 with the black arrows indicating the connections of TP's low clouds to global water

368 vapor in the upper troposphere with high frequencies.

369

370

371

372

373

374

375

376

377

378

379

380

381

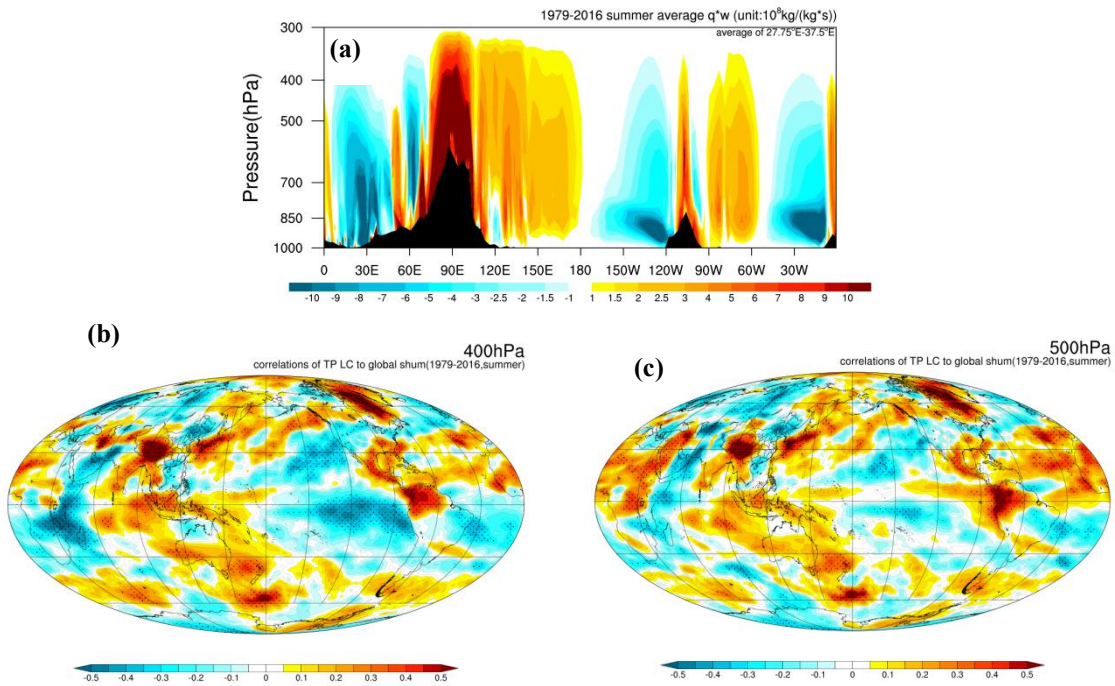
382

383

384

385

386



387 **Figure 2.** (a) The vertical section of vertical vapor transport flux averaged over 27.5-
 388 32.0°N in summers of 1979-2016; the spatial distributions of correlation coefficients of
 389 low cloud cover over the TP with the global specific humidity of the ECMWF-interim
 390 data in Summer (June, July and August) from 1979 to 2018 at (b) 400hPa and (c) 500hPa.

391

392

393

394

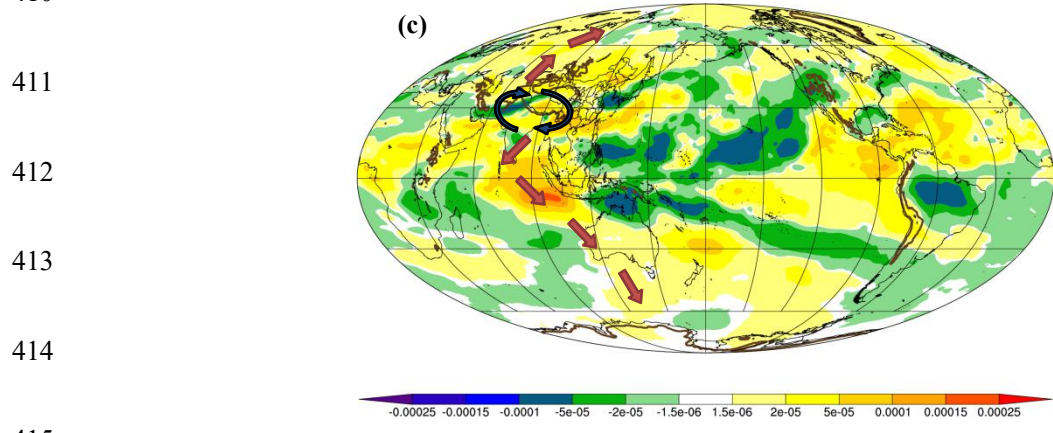
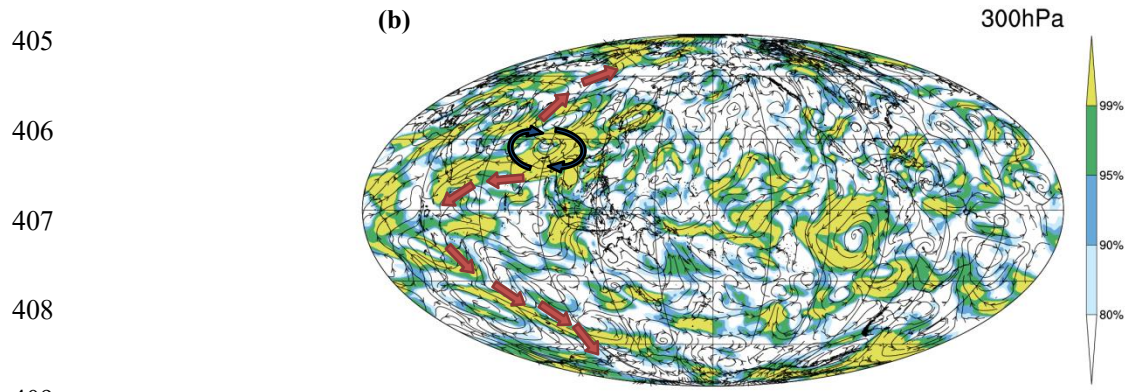
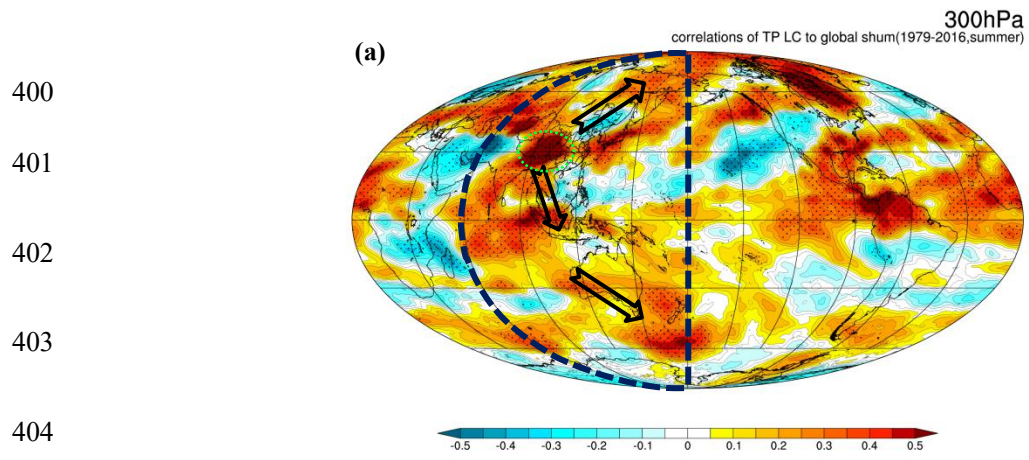
395

396

397

398

399



416
417
418
419

420

421

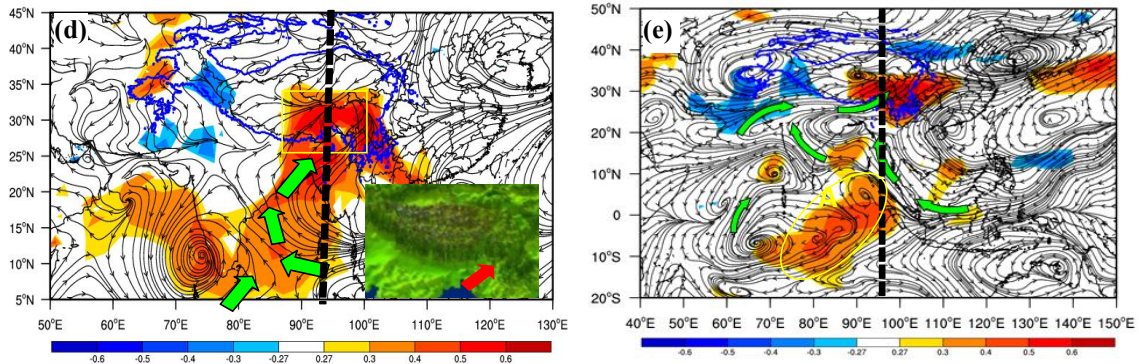
422

423

424

425

426



427

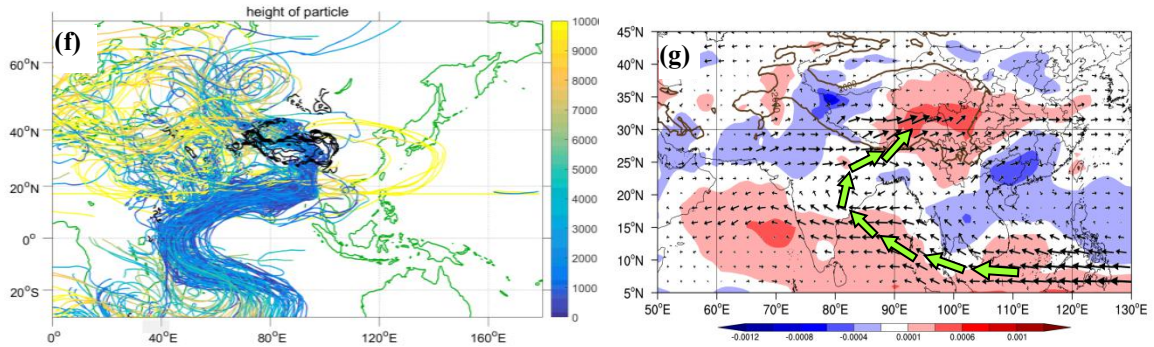
428

429

430

431

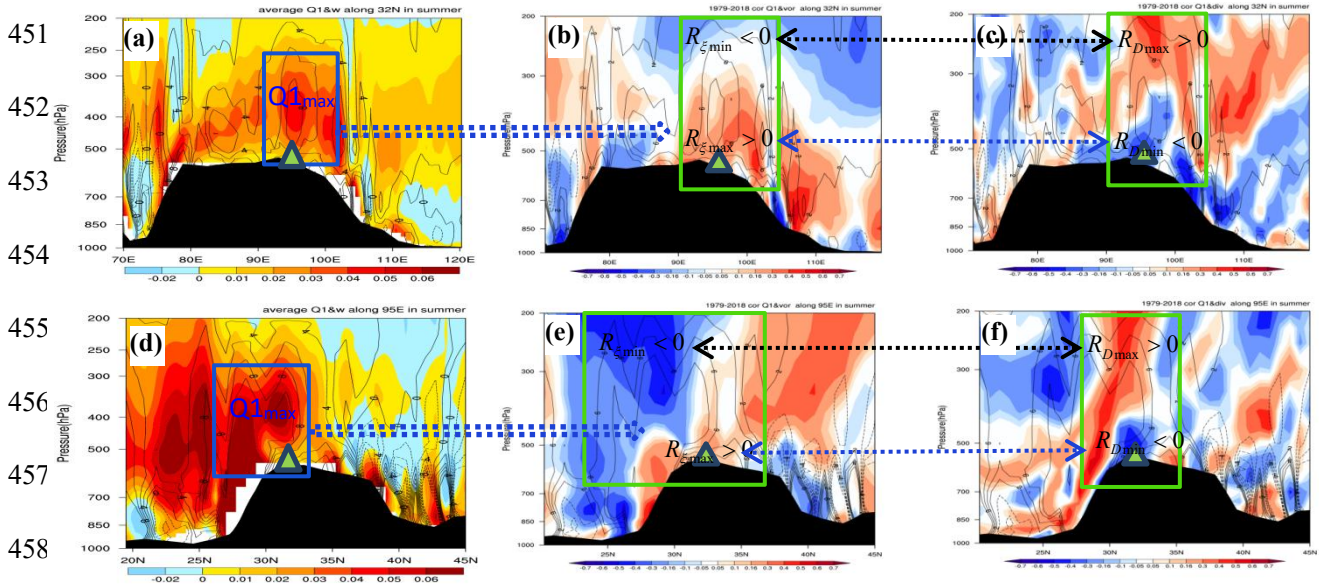
432



433 **Figure 3.** (a) The spatial distributions of correlation coefficients of low cloud cover over the TP
 434 with the global specific humidity of the ECMWF-interim data at 300 hPa in summers of 1979-
 435 2016 with the pathways of convective air to the troposphere; (b) correlation vectors of the
 436 column Q_1 integrated vertically over the TP region (80-102°E; 30-37.5°N) with the 300hPa vapor
 437 transport flux in July of 2014-2016, The shaded area indicates the correlation coefficient passing
 438 the the 90% confidence level; (c) the difference of specific humidity (shading, unit:kg/kg) at 300
 439 hPa in summer in 1998 and 2007 with anomalously high Q_1 and in 1997 and 2003 with
 440 anomalously low Q_1 in the AWT, The black and orange arrows indicate respectively the
 441 anticyclonic circulations in the TP and water vapor transport pathways from the TP to the Arctic
 442 and Antarctic regions.; the correlation field between the total apparent heat source Q_1 over the TP
 443 region (80-102°E; 30-37.5°N) with the water vapor (shaded) and water vapor flux (stream lines)

444 in the surface layer (d) and middle layer (500hpa) (e) in summer over 1979-2015, respectively, (f)
 445 the backward trajectories of water vapor transport simulated with the model FLEXPART in July,
 446 2009. (g) the difference of vapor transport flux at 500 hPa (vectors, unit:gs⁻¹hPa⁻¹cm⁻¹) and
 447 specific humidity (color contours, unit:kg/kg) between summers with anomalously high Q₁ in
 448 1998, 2005, 2007, 2008 and 2009 and with anomalously low Q₁ in 1994, 1997, 2001, 2002 and
 449 2003 over the TP

450



459

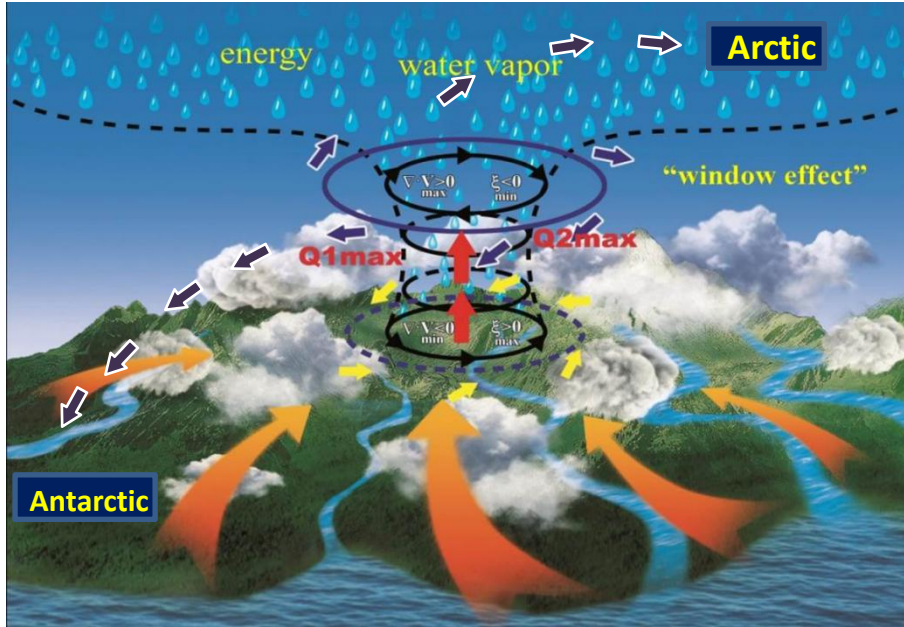
460 **Figure 4.**The vertical sections of (a,d) vertical motion (contours, in unit: $10^{-2}\text{Pa}\cdot\text{s}^{-1}$) and Q₁
 461 (color contours, in unit: 10^{-3}w kg^{-1}); (b,e) vertical motion (contours, in unit: $10^{-2}\text{Pa}\cdot\text{s}^{-1}$) and
 462 correlation coefficients (color contours) between Q₁ and the vorticity as well as (c,f) vertical
 463 motion (contours, in unit: $10^{-2}\text{Pa}\cdot\text{s}^{-1}$) and the correlation coefficients between Q₁ and the
 464 divergence (contours) in the TP, with Figs. a, b and c along 32 °N, and Figs. d, e and f along 95
 465 °E. The green triangles indicate the AWT core region.

466

467

468

469



470

471 **Figure 5.** A diagram of vertical water vapor transport in the troposphere driven by the
472 thermal forcing of AWT over the TP, where the vertical transport window of water vapor
473 in the troposphere connects globally the water vapor transport from the tropical oceans
474 and the southern Indian Ocean in the lower troposphere with transport to the Arctic and
475 Antarctic regions in the upper troposphere.

476

477

478